Manuscript accepted for publication in *Geophysical Research Letters*

Phosphine in the Venusian Atmosphere: A Strict Upper Limit from SOFIA GREAT Observations

M. A. Cordiner[1,2], G. L. Villanueva[1], H. Wiesemeyer[3], S. N. Milam[1], I. de Pater[4], A. Moullet[5], R. Aladro[3], C. A. Nixon[1], A. E. Thelen[1], S. B. Charnley[1], J. Stutzki[3], V. Kofman[1], S. Faggi[1], G. Liuzzi[1,6], R. Cosentino[7], B. A. McGuire[8]

[1]Solar System Exploration Division, NASA Goddard Space Flight Center, 8800 Greenbelt Road, Greenbelt, MD 20771, USA.
[2]Department of Physics, Catholic University of America, Washington, DC 20064, USA.
[3]Max Planck Institute for Radio Astronomy, Auf dem Hügel 69, D-53121 Bonn, Germany.
[4]Department of Astronomy, University of California, 501 Campbell Hall, Berkeley, CA 94720-3411, USA.
[5]NASA Ames Research Center, Moffett Field, CA 94035, USA.
[6]School of Engineering, Università degli Studi della Basilicata, 85100, Potenza, Italy
[7]Space Telescope Science Institute, Baltimore, MD 21218, USA.
[8]Department of Chemistry, Massachusetts Institute of Technology, Cambridge, MA 02139, USA.

Key Points:

- A recent detection of phosphine (a possible biomarker) on Venus at millimeter wavelengths has been called into question by subsequent work.
- We performed far-infrared spectroscopic observations of Venus using the GREAT instrument onboard the SOFIA aircraft.
- Phosphine was not detected, and a strict upper limit on its atmospheric abundance of 0.8 ppb was derived between 75–110 km.

Corresponding author: M. A. Cordiner, martin.cordiner@nasa.gov

Abstract
The presence of phosphine (PH_3) in the atmosphere of Venus was reported by Greaves et al. (2021a), based on observations of the J =1–0 transition at 267 GHz using ground-based, millimeter-wave spectroscopy. This unexpected discovery presents a challenge for our understanding of Venus's atmosphere, and has led to a reappraisal of the possible sources and sinks of atmospheric phosphorous-bearing gases. Here we present results from a search for PH_3 on Venus using the GREAT instrument aboard the SOFIA aircraft, over three flights conducted in November 2021. Multiple PH_3 transitions were targeted at frequencies centered on 533 GHz and 1067 GHz, but no evidence for atmospheric PH_3 was detected. Through radiative transfer modeling, we derived a disk-averaged upper limit on the PH_3 abundance of 0.8 ppb in the altitude range 75–110 km, which is more stringent than previous ground-based studies.

1 Introduction

Greaves et al. (2021a) presented the first evidence for phosphine (PH_3) gas on Venus, based on a tentative detection of the J = 1–0 line at 267 GHz using the James Clerk Maxwell Telescope (JCMT), in addition to a seemingly more convincing detection of the same line using the Atacama Large Millimeter/submillimeter Array (ALMA), at a formally-derived statistical significance of 15σ (Figure 1). A disk-averaged PH_3 abundance of 20 ppb was obtained by Greaves et al. (2021a), but following recalibration of the ALMA data, a smaller value in the range $\sim$ 1–7 ppb was derived (Greaves et al., 2021b). The claimed detection of PH_3 was surprising considering the difficulty of producing this gas from abiotic mechanisms such as atmospheric photochemistry, geochemistry or meteorological processes (Greaves et al., 2021a; Bains et al., 2021a), which led to speculation regarding a possible biological origin. The potential utility of PH_3 as a biomarker (indicator for the presence of life) in planetary and exoplanetary atmospheres is presently under investigation (Sousa-Silva et al., 2020; Wunderlich et al., 2021). However, theorizing and speculation regarding the origin of Venusian PH_3 at parts-per-billion levels remains premature, considering several problems have been identified with the Greaves et al. (2021a) data calibration and analysis procedures by multiple, independent studies (Snellen et al., 2020; Villanueva et al., 2021; Thompson, 2021; Lincowski et al., 2021; Akins et al., 2021). In contrast to Greaves et al. (2021a), these subsequent investigations found no significant evidence for PH_3 absorption in the same JCMT and ALMA data. The tentative JCMT detection can be explained as a statistical outlier, amplified/introduced by repeated subtraction of fitted, periodic baseline ripples, whereas the significance of the initial ALMA detection is reduced to (at or near) zero when conventional bandpass calibration procedures are applied. It was further shown by Villanueva et al. (2021) that the presence (or not) of a putative absorption feature at the PH_3 J = 1–0 frequency is dependent on the order of polynomial used in the baseline subtraction, making it difficult to obtain a reliable PH_3 detection from those data.

The JCMT and ALMA (disk-averaged) spectra from Greaves et al. (2021a) and Greaves et al. (2021b) are compared with three different, standard, reduction methods for the same ALMA data in Figure 1 (see Villanueva et al. (2021) for further details). The Venus atmospheric model for a PH_3 abundance of 1 ppb (the upper limit derived by Villanueva et al. (2021)) is also overlaid on top of the red curve.

Follow-up attempts to detect PH_3 on Venus using infrared spectroscopy were performed using archival data from the NASA Infrared Telescope Facility (IRTF) on Hawaii (Encrenaz et al., 2020), and from the Venus Express orbiter (Trompet et al., 2021). These studies were sensitive to PH_3 in the altitude range $\sim$ 60–95 km, but no phosphine was detected. On the other hand, a reanalysis of Pioneer Venus mass spectrometry data by Mogul et al. (2021) revealed peaks at masses (per unit charge)

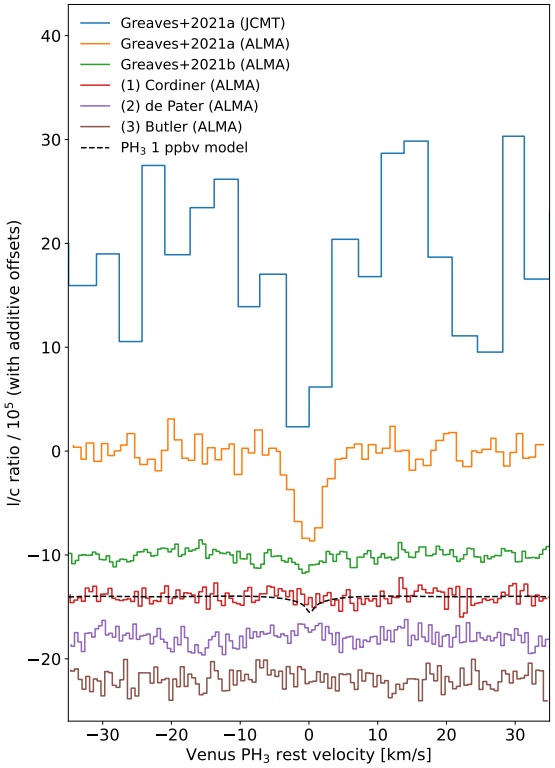

Figure 1. JCMT and ALMA spectra from the original Venus study of Greaves et al. (2021a) (top two traces), showing the spectral region in the vicinity of the PH_3 $J = 1–0$ line at 266.945 GHz. The lower four traces show disk-averaged ALMA spectra derived from the same data using different calibration and reduction methodologies by different authors, as explained by Villanueva et al. (2021) and Greaves et al. (2021b). For reference, the black dashed trace shows the 1 ppb PH_3 spectral model (upper limit) from Villanueva et al. (2021). The Greaves et al. (2021a) and (2021b) ALMA spectra differ considerably, due to improper calibration of the 2021a data.

of 33.997 amu/q and 32.989 amu/q, consistent with the presence of PH_3^+ and PH_2^+, respectively, at an altitude of 51.3 km. However, the close overlap of these mass peaks with H_2S^+ (33.988 amu) and HS^+ (32.980) introduces ambiguity into these molecular detections. Furthermore, the detection of (ionized) atomic P^+ by Mogul et al. (2021) was of marginal significance, considering the error bars. Meanwhile, further analysis by Greaves et al. (2022) of the original ALMA and JCMT data continues to support the case for PH_3 being present in the atmosphere of Venus.

To help resolve the debate concerning the possible presence of phosphine on Venus, we performed spectroscopic observations using the Stratospheric Observatory for Infrared Astronomy (SOFIA) targeting multiple rotational transitions of PH_3 at high sensitivity and high spectral resolution. Due to its operating altitude of around 13 km, SOFIA has unique access to high-frequency submillimeter and infrared emission, which is not accessible using ground-based astronomy due to the opacity of Earth's atmosphere at these wavelengths. Our aim was to detect a set of the stronger, higher-energy rotational transitions of collisionally-excited PH_3, to augment prior observations and provide a robust measure of the PH_3 abundance in Venus's atmosphere. By virtue of the extremely high spectral resolution of the SOFIA heterodyne instrument (up to $R = 4 \times 10^6$ at 1067 GHz), our observations provide altitudinal sensitivity for phosphine in the range 75–110 km, extending to higher altitudes than Encrenaz et al. (2020) and Trompet et al. (2021), with global coverage of Venus. Our new study therefore provides spatial coverage that is highly complementary to the PH_3 upper limits obtained previously at shorter infrared wavelengths.

2 Materials and Methods

2.1 Observations

Observations were performed using the German REceiver for Astronomy at Terahertz Frequencies (GREAT), on the SOFIA telescope, over three flights conducted on UT 2021-11-10, 12 and 13 as part of Director's discretionary time program #75_0059. During this time, Venus was at a geocentric distance of 0.58 au, with an angular diameter of 28″ and a solar illumination phase of 98°–100°. The total integration time on Venus was 36 minutes.

GREAT is a modular-design heterodyne spectrometer operating at submillimeter and far-infrared wavelengths. For this experiment, the "4GREAT" instrument setup was used (Duran et al., 2021), consisting of four single-pixel mixers, out of which the first two units — 4G1 and 4G2 (carrying superconductor-insulator-superconductor mixers and operating at frequencies around 0.5 and 1.0 THz, respectively) — were used to target phosphine.

Typical single-sideband receiver temperatures for 4G1 and 4G2 were 230 K and $\sim$ 1000 K, respectively. The zenith precipitable water vapor column was close to 0.02 mm for all three flights, and the corresponding zenith opacities were $\sim$ 0.12 in both bands. The mean aircraft altitude was 12.2 km. Total system temperatures were 350–370 K for 4G1 and 1100–1570 K for 4G2, increasing during each flight due to the decreasing elevation angle of Venus (typically from 21° to 16°).

The total power signal due to Earth's atmosphere was removed from the spectra by fast-chopping (at 0.6 Hz), alternating between two opposing reference positions 3′ away from the science target. Telescope guiding was achieved by targeting Venus's opto-center, which resulted in an 8″ offset in the science pointing position away from the geometric center of the planet's disk. The raw spectroscopic data were calibrated to Rayleigh-Jeans equivalent brightness temperatures using calibration loads at ambient and cold temperatures ($\approx$ 300 K and 68 K, respectively).

The extended fast Fourier transform spectrometers (Klein et al., 2012) cover an intermediate-frequency (IF) base-band ranging from 4 to 8 GHz, utilizing 16,384 frequency channels, resulting in a generic spectral resolution of 244 kHz. The 4G1 and 4G2 local oscillator frequencies were configured to simultaneously observe the PH_3 $J = 2 - 1$ doublet at 534 GHz (in the 4G1 lower sideband; LSB) and the PH_3 $J = 4 - 3$ quadruplet at 1067 GHz (in the 4G2 upper sideband; USB). The SOFIA beam FWHM was $54''$ for the 4G1 channel and $25''$ for 4G2. The spectral axis was Doppler-corrected to the Venus rest frame, and later rebinned by a factor of four (to a spectral resolution of 976 kHz) for subsequent data analysis. Individual line frequencies and basic spectroscopic parameters are given in Table S1, including the Einstein A coefficient, the upper-state statistical weight (g_u), and the upper-state energy (E_u) of each transition.

2.2 Telluric Modeling and Continuum Fringe Removal

The observed Venus spectra (Figure 2), are composed of a linear combination of contributions from the upper and lower receiver sidebands, in a ratio of approximately 1 : 1. The resulting spectra are dominated by the Venus thermal continuum, which is overlaid by several deep absorption lines due to terrestrial (telluric) ozone (O_3). A quasi-periodic fringe pattern is also evident in the continuum of both the 4G1 and 4G2 bands, with an amplitude of about 0.7% of the continuum level, and an appearance characteristic of multiple overlapping sine waves of different frequencies. These fringes arise primarily due to internal reflections between the hot and cold calibration loads and the SOFIA subreflector, further modulated by the interfering contributions from the two sidebands (LSB + USB) in each receiver channel, and are therefore nontrivial to characterize (see Supporting Information text, Section S1).

Fourier analysis is a valid approach for identifying and removing such periodic spectral components, but for the present study, we adopt an iterative Lomb-Scargle 'periodogram' method (Scargle, 1982). This involves cross-correlating the observed spectra with a set of sine waves spanning a broad, quasi-continuous range of angular frequencies ($\omega = 2\pi/T_\nu$, where T_ν is the wave period in frequency space). The peak cross-correlation amplitude is then plotted as a function of ω to produce the periodogram. Specific ω values were identified from the global maxima of the periodogram, and their corresponding sine waves were fitted one-by-one to the observed spectrum, optimizing the wave phases and amplitudes using least-squares minimization. The individual waves were subtracted sequentially from the observed spectra, and the periodogram was regenerated after each iteration. Our iterative fringe removal procedure was terminated when no further clear periodic signals could be identified in the data, which occurred after seven iterations for both the 4G1 and 4G2 channels (see Supporting Information Figures S1 and S2).

The Lomb-Scargle periodigram method provides a more nuanced approach than Fourier analysis, since it identifies and removes a single, fully characterized sine-wave component at each step, whereas Fourier analysis tends to be more destructive, removing a broader range of harmonics, with poorly-characterized phases and amplitudes. The Lomb-Scargle method also works with masked data, which helps prevent accidental removal of real spectral features. Furthermore, an identical set of wave components can be removed from the observations and from the spectral models for Venus, which allows investigation of the degree to which various (real) atmospheric signals may be corrupted as a result of continuum fringe removal.

For optimal removal of the instrumental fringes using this method, it is necessary to work with a baseline-subtracted spectrum, with the continuum and telluric lines removed. The fitted (continuum + telluric) model is later added back to the de-fringed spectra to facilitate subsequent analysis. A spectral model for Venus (as

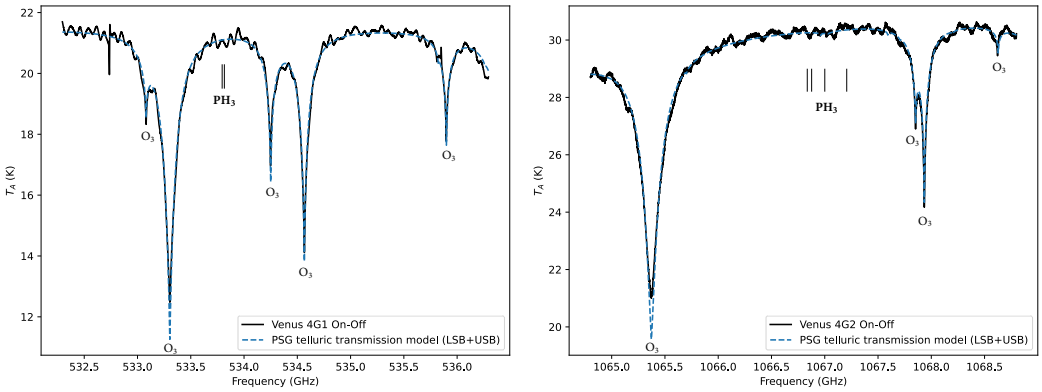

Figure 2. SOFIA Venus spectra from the 4G1 (left) and 4G2 (right) channels of the GREAT receiver. PSG terrestrial transmission models are overlaid, highlighting the presence of strong telluric O_3 absorptions. The spectra contain overlapping contributions from the lower and upper receiver sidebands. Vertical bars indicate PH_3 line frequencies.

viewed through Earth's atmosphere), was therefore constructed using the Planetary Spectrum Generator (PSG) (Villanueva et al., 2018), following the same methodology as Villanueva et al. (2021), using gas abundance data from Ehrenreich et al. (2012) and the VIRA-45 temperature profile of Zasova et al. (2006). Our model geometry specifically accounts for the size and offset of the SOFIA beam with respect to Venus (see Section 2.1). The resulting model spectra for the upper and lower sidebands of the 4G1 and 4G2 channels were multiplied by corresponding PSG models for the terrestrial transmittance in the direction of Venus at the time of our SOFIA observations, taking into account the aircraft's mean latitude, longitude, altitude, and velocity along the line of sight. For each 4GREAT channel, the two model spectra for each sideband were overlaid and averaged together. A uniform scaling factor of 0.72 was applied to the terrestrial O_3 vertical abundance profile to obtain the best fit to the observed spectra, shown with dashed blue curves in Figure 2. A linear (multiplicative) gain slope was also included in the spectral model fits, to account for the varying 4GREAT amplitude response as a function of frequency.

During fitting of the continuum, as well as for subsequent removal of the instrumental fringes, the spectral regions within ± 5 km s^{-1} of the PH_3 lines were masked, therefore avoiding biasing the fit as a result of the presence (or absence) of PH_3, which was not included in the Venus atmospheric model at this stage. Due to the severity of telluric O_3 absorption in our spectra, and the difficulty in obtaining a perfect fit to the cores of the deepest telluric lines, we chose to perform all subsequent analysis (including fringe removal) on a restricted frequency range of ± 100 km s^{-1} either side of the PH_3 lines (533.4–534.1 GHz for 4G1 and 1066.3–1067.7 GHz for 4G2), where the continuum fit was sufficiently good.

3 Results

Observed, de-fringed SOFIA spectra in the vicinity of the targeted PH_3 lines are shown in Figure 3. The RMS noise is 24 mK for the 4G1 spectra and 59 mK for 4G2, which is reasonably close to the theoretical values of 14 mK and 50 mK, respectively. The locations of the PH_3 lines are labeled, and for the 4G2 channel, broad contaminating lines due to telluric O_3 and NO_2 are also identified. These contaminants originate at rest frequencies of 1078.686 GHz and 1078.621 GHz in the upper 4G2

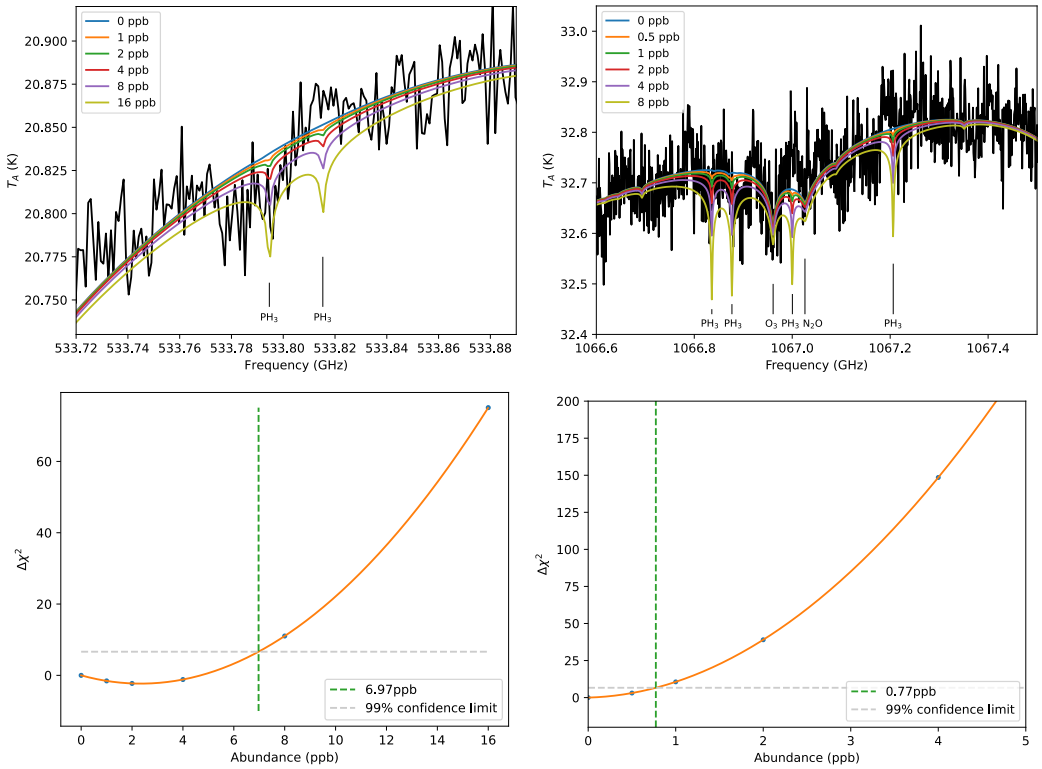

Figure 3. SOFIA GREAT Venus spectra in the 4G1 (top left) and 4G2 (top right) channels (shown in black). A family of PSG models is overlaid for each channel (coloured curves), spanning a range of different PH_3 abundances as identified in the legend. Major spectral features are labeled. Lower panels show the corresponding $\Delta\chi^2$ curve for each channel; the abundances corresponding to the 99% confidence limit (*i.e.* $\Delta\chi^2 = 6.63$) are highlighted with green dashed lines.

sideband, and are present in both the observed and modeled spectra. Several other, weaker lines due to terrestrial O_3 contamination are visible in the 4G2 model spectra, but these have not been labeled. No clearly-identifiable PH_3 lines can be seen in either the 4G1 or the 4G2 frequency ranges.

We performed a statistical analysis to quantify the amount of PH_3 that could be present in Venus's atmosphere, given the noise level of our data. A set of spectral models was generated as in Section 2.2, consisting of Venus + telluric spectra for the LSB and USB in each 4GREAT channel, including (for Venus) CO_2, N_2, CO, O_2, SO_2, H_2O, O_3, He and PH_3 gases. Starting with a PH_3 abundance of zero, and with the ± 5 km s^{-1} regions surrounding the PH_3 lines masked, the model Venus continuum was scaled to obtain the best fit to the observations. Using a constant PH_3 abundance with altitude, the amount of PH_3 in the model was steadily increased, and the difference between the model and observations was monitored using the χ^2 statistic (*e.g.* Nixon et al. (2010)). The change in χ^2 as a function of the PH_3 abundance a ($\Delta\chi^2(a) = \chi^2(a) - \chi^2_0$, where χ^2_0 is the chi-square value at $a = 0$) is plotted for 4G1 and 4G2 in the lower panels of Figure 3.

For 4G1, a minimum in the chi-square curve occurs at a PH_3 abundance of $a = 2.3$ ppb, for which $\Delta\chi^2$ is -2.3. This corresponds to only a 1.5σ confidence interval, and is therefore not a significant detection. The 99% statistical confidence limit is reached for $a = 6.97$ ppb, which we consider to be a robust upper limit on the PH_3 abundance for this (4G1) channel. The PH_3 lines in the 4G2 channel provide a more sensitive upper limit than 4G1 due to their larger Einstein A values and statistical weights (Table S1), in addition to higher energy level populations in the atmospheric regions we are probing. The $\Delta\chi^2$ curve for 4G2 is at a minimum for $a = 0$ and rises to reach the 99% confidence threshold at $a = 0.77$ ppb. This represents a stringent upper limit on the average PH_3 abundance within the 4G2 beam.

The 4G1 PH_3 upper limit represents a robust disk-averaged measurement due to the relatively large beam size ($54''$) compared with Venus's $28''$ disk. On the other hand, the smaller ($25''$) 4G2 beam — offset $8''$ from Venus's disk-center — integrates only 56% of the total planetary disk emission (assuming spatially-uniform emission), and primarily samples dayside (afternoon) equatorial latitudes. Adopting the low-latitude ($\phi < 35°$) VIRA temperature profile for the Venusian afternoon (solar time 13:30–18:00) from Zasova et al. (2006), results in a 4% increase in the modeled beam-averaged PH_3 ($J = 4 - 3$) line depths relative to the continuum. Consequently, the PH_3 upper limit from 4G2 may be further reduced to $a = 0.74$ ppb. In reality, due to the Gaussian beam shape (with its broad wings extending over the entire planet), our observations are sensitive to a somewhat broader range of latitudes and solar times, so the true upper limit should be in the range $a = 0.74$–0.77 ppb. An additional error margin of a few per-cent should also be included, considering uncertainties in the adopted VIRA temperature profiles. A more accurate upper limit would therefore be obtained using actual temperature measurements for the global Venusian atmosphere, contemporaneous with our observations, but in the absence of such data, we conservatively round the PH_3 abundance upper limit up to 0.8 ppb.

4 Discussion

Our upper limit represents confirmation of the ~ 1 ppb upper limit derived by Villanueva et al. (2021) using the Greaves et al. (2021a) ALMA data (based on a spatially-filtered average of the Venusian disk), but is at odds with the 20 ppb derived by Greaves et al. (2021a) using JCMT spectra. Although we cannot rule out temporal variability of the putative PH_3 signal, our result is consistent with the findings of Thompson (2021), who determined that the PH_3 absorption identified by Greaves et

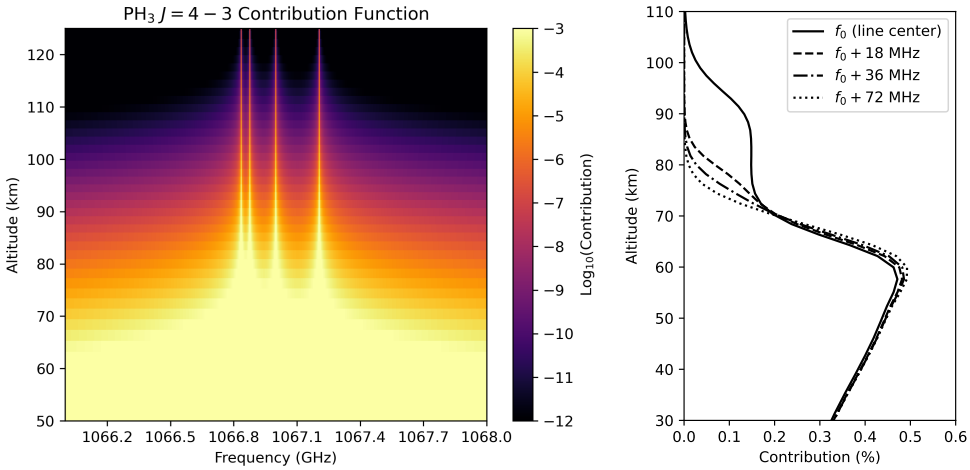

Figure 4. Left panel: contribution function from our Venus radiative transfer model, showing the fraction of the total spectral opacity as a function of frequency and altitude for the 4G2 band. The four prominent peaks are due to the PH$_3$ $J_K = 4_K - 3_K$ lines (see Table S1). Right panel: one-dimensional cuts through the contribution function for the highest-frequency ($J_K = 4_3 - 3_3$) PH$_3$ line, at various frequency offsets from the line core frequency ($f_0 = 1067.2063$ GHz).

al. (2021a) in their JCMT spectra may have been an artifact resulting from high-order polynomial baseline correction.

Our SOFIA data also suffer from significant baseline ripples (fringes). It is therefore important to evaluate the degree to which our results may have been affected by our fringe removal strategy. Masking the PH$_3$ lines of interest during fringe removal was a crucial initial step to help avoid accidental fitting and removal of any real PH$_3$ signal. The masked regions (± 5 km s^{-1}; 18 MHz either side of each 4G2 PH$_3$ line) were selected to mark the approximate boundary for where the pressure-broadened model PH$_3$ lines become difficult to distinguish from the continuum. Care was also taken to ensure these regions were narrow enough to leave enough continuum visible for reliable periodogram generation (see Figures S1 and S2).

Figure S3 shows a demonstration that our defringing method has no significant impact on the strengths of the narrow parts of the PH$_3$ lines (within the ± 5 km s^{-1} masked regions). These figures were generated by fitting and removing from the models in sequence, the same set of periodic waves as identified for the observed spectra (Section 2.2), by varying their amplitudes but keeping their phases and ω values fixed. At each step, the best-fitting sine wave was subtracted until all seven frequency components were removed. Some minor distortion of the broad line wings and continuum is evident, but this is well below the noise level (as shown in the lower panels of Figure S3). Consequently, our abundance analysis is expected to be reliable for absorption originating from the narrow PH$_3$ line core regions.

The full spectral contribution function from our 4G2 Venus radiative transfer model is shown in Figure 4. The contribution function includes all species in the model, and reveals that the narrow PH$_3$ $J = 4$ spectral line cores only begin to become readily distinguishable from the heavily-broadened line wings for altitudes above 70 km. The right panel of Figure 4 shows more clearly the vertical behaviour of the $J_K = 4_3 - 3_3$ line core absorption compared with the wings, with similar amounts of absorption

from the line core (f_0) and various line wing positions for altitudes $\lesssim$ 70 km. The $f_0 \pm 18$ MHz window to which our SOFIA observations are most sensitive corresponds to spectroscopically distinct absorption in the altitude range $\approx$ 75–110 km. This is significantly higher than the $\sim$ 60–70 km range probed by the infrared observations of Encrenaz et al. (2020), who obtained $a < 5$ ppb; our SOFIA observations are therefore consistent with that study, but provide a complementary, stricter upper limit at higher altitudes.

Our 0.8 ppb upper limit is also consistent with Trompet et al. (2021), who obtained phosphine upper limits less than 20 ppb from various Venus Express solar occultation measurements in the altitude range 60–95 km. Their strictest upper limits ($\lesssim$ 1 ppb) were obtained at latitudes within about 20 degrees of Venus's poles, and in the altitude range 60–77 km; their lowest value being 0.2 ppb at 69 km. Consequently, our SOFIA observations, by virtue of being more sensitive to equatorial latitudes, as well as higher altitudes, are again, highly complementary to these previous observations.

We also generated contribution functions for the PH_3 $J = 1$–0 line (the same one observed by Greaves et al. (2021a) using ALMA and JCMT), as shown in figure S4. Due the lower energy of the $J = 1$ level ($E_u = 13$ K, *vs.* 121 K for $J = 4_3$), the Greaves et al. (2021a) observations sound slightly higher altitudes, a few kilometers above our SOFIA observations. Figure S4 (right panel) also shows that the continuum-subtracted spectral region within ± 5 km s^{-1} (± 4.5 MHz) of the PH_3 $J = 1$–0 line is only sensitive to emission from above 75 km. This is significantly higher than the altitude of Venus's cloud tops (around 60–70 km), and is at odds with the claim by Greaves et al. (2021a) that they detected PH_3 in the cloud decks.

The non-detection of PH_3 by several teams confirms a strict upper limit on the phosphine gas abundance across a range of latitudes within the mid-to-upper atmosphere of Venus. Conversely, strong evidence for the presence of other phosphorous-bearing compounds in Venus's atmosphere was provided by X-ray radiometry of aerosol particles by the Vega-1 and Vega-2 descent probes (Andreichikov et al., 1987). Surprisingly, in the altitude range 47–52 km, the cloud aerosols were found to consist primarily of P-bearing compounds, while between 52–62 km, they were dominated by sulfur- and chlorine-containing species. Based on lithospheric chemical abundance arguments, Andreichikov (1987) therefore deduced that phosphorous oxides and phosphoric acids were a likely component of the Venusian cloud particles, plausibly generated from the condensation of volcanic vapors. The participation of phosphorous oxides (P_nO_m) in atmospheric chemical processes in the cloud layers, including reaction with H_2SO_4 and other sulphur-bearing species in the presence of H_2O, can result in the production of phosphoric acid and HPO-bearing polymers (Andreichikov, 1987; Krasnopolsky, 1989). A complex chemical network involving phosphorous on Venus is therefore in effect. However, the plausibility of forming PH_3 as a result of Venus photochemistry was explored by Bains et al. (2021b), and no efficient chemical pathways have yet been found. The possible production of detectable quantities of PH_3 in and above the clouds, as a result of phosphide release from volcanic plumes (Truong & Lunine, 2021), also remains questionable (Bains et al., 2022), so the non-detection of PH_3 gas is not surprising given our current knowledge.

5 Conclusions

SOFIA GREAT spectra of the PH_3 $J = 2$–1 and 4–3 transitions obtained toward Venus on 2021 November 10th–13th show no significant evidence for the presence of phosphine gas. From our most sensitive observations (in the 4G2 channel), we derived an upper limit on the PH_3 abundance of 0.8 ppb in the altitude range $\approx$ 75–110 km. The 25″ telescope beam, pointing at the Venus opto-center, was sensitive to emission

from across the entire disk of Venus, but with a peak sensitivity in the vicinity of the dayside equator. As a result of our high spectral-resolution observations, combined with previous infrared studies using Venus Express and IRTF, we now have in-hand a robust body of evidence demonstrating a lack of phosphine gas in Venus's atmosphere, spanning a broad range of altitudes $\sim 60 - 110$ km, with latitudinal coverage ranging from equatorial to polar.

Our measurements, obtained around a single epoch, do not rule out the possibility of time-variability in the Venus PH_3 abundance. Due to its utility as a possible indicator for unexpected geological, atmospheric, and biological processes, there is merit in continued searches for PH_3 in the atmospheres of Venus and other planets. Further theoretical and laboratory-based investigations of phosphorous chemistry in solid, liquid and vapor phases will also be required, to better understand the planetary sources and sinks of this biologically important element.

6 Open Research

All observational data used in this study are freely available from the SOFIA science archive at https://irsa.ipac.caltech.edu/applications/sofia using AOR ID 75_0059_1.

Data reduction and analysis scripts (written in Python 3) are accessible from the Zenodo repository (Cordiner, 2022).

The Planetary Spectrum Generator (PSG) used for producing our spectral models is accessible at psg.gsfc.nasa.gov.

Acknowledgments
This work is based on observations made with the NASA/DLR Stratospheric Observatory for Infrared Astronomy (SOFIA). SOFIA is jointly operated by the Universities Space Research Association, Inc. (USRA), under NASA contract NNA17BF53C, and the Deutsches SOFIA Institut (DSI) under DLR contract 50 OK 2002 to the University of Stuttgart. Financial support for this work was provided by NASA through award #75_0059 issued by USRA. Research at NASA GSFC was also supported by the NASA Planetary Science Division Internal Scientist Funding Program through the Fundamental Laboratory Research work package (FLaRe). The German Receiver for Astronomy at Terahertz Frequencies GREAT (Risacher et al., 2018) is a development by the MPI für Radioastronomie and the KOSMA Universität zu Köln, in cooperation with the MPI fürSonnensystemforschung and the DLR Institut für Planetenforschung. We gratefully acknowledge support from the GREAT team in setting up and performing the observations.

References

Akins, A. B., Lincowski, A. P., Meadows, V. S., & Steffes, P. G. (2021, February). Complications in the ALMA Detection of Phosphine at Venus. *ApJL*, *907*(2), L27. doi: 10.3847/2041-8213/abd56a

Andreichikov, B. M. (1987, September). Chemical composition and structure of Venus clouds from results of X-ray radiometric experiments made with the Vega 1 and Vega 2 automatic interplanetary stations. *Kosmicheskie Issledovaniia*, *25*, 737-743.

Andreichikov, B. M., Akhmetshin, I. K., Korchuganov, B. N., Mukhin, L. M., Ogorodnikov, B. I., Petryanov, I. V., & Skitovich, V. I. (1987, September). Chemical composition and structure of Venus clouds from results of X-ray radiometric experiments made with the Vega 1 and Vega 2 automatic interplanetary stations. *Kosmicheskie Issledovaniia*, *25*, 721-736.

Bains, W., Petkowski, J. J., Seager, S., Ranjan, S., Sousa-Silva, C., Rimmer, P. B., ... Richards, A. M. S. (2021a, October). Phosphine on Venus Cannot Be Explained by Conventional Processes. *Astrobiology*, *21*(10), 1277-1304. doi: 10.1089/ast.2020.2352

Bains, W., Petkowski, J. J., Seager, S., Ranjan, S., Sousa-Silva, C., Rimmer, P. B., ... Richards, A. M. S. (2021b, October). Phosphine on Venus Cannot Be Explained by Conventional Processes. *Astrobiology*, *21*(10), 1277-1304. doi: 10.1089/ast.2020.2352

Bains, W., Shorttle, O., Ranjan, S., Rimmer, P. B., Petkowski, J. J., Greaves, J. S., & Seager, S. (2022, February). Only extraordinary volcanism can explain the presence of parts per billion phosphine on Venus. *Proceedings of the National Academy of Science*, *119*(7), e2121702119. doi: 10.1073/pnas.2121702119

Cordiner, M. (2022, August). Data analysis scripts for submitted article "Phosphine in the Venusian Atmosphere: A Strict Upper Limit from SOFIA GREAT Observations" [Software]. *Zenodo*. Retrieved from `https://doi.org/10.5281/zenodo.7020418` doi: 10.5281/zenodo.7020418

Duran, C. A., Gusten, R., Risacher, C., Gorlitz, A., Klein, B., Reyes, N., ... Lis, D. C. (2021, March). 4GREAT—A Four-Color Receiver for High-Resolution Airborne Terahertz Spectroscopy. *IEEE Transactions on Terahertz Science and Technology*, *11*(2), 194-204. doi: 10.1109/TTHZ.2020.3042714

Ehrenreich, D., Vidal-Madjar, A., Widemann, T., Gronoff, G., Tanga, P., Barthélemy, M., ... Arnold, L. (2012, January). Transmission spectrum of Venus as a transiting exoplanet. *Astron. Astrophys*, *537*, L2. doi: 10.1051/0004-6361/201118400

Encrenaz, T., Greathouse, T. K., Marcq, E., Widemann, T., Bézard, B., Fouchet, T., ... Sousa-Silva, C. (2020, November). A stringent upper limit of the PH_3 abundance at the cloud top of Venus. *Astron. Astrophys.*, *643*, L5. doi: 10.1051/0004-6361/202039559

Greaves, J. S., Richards, A. M. S., Bains, W., Rimmer, P. B., Clements, D. L., Seager, S., ... Fraser, H. J. (2021b, January). Reply to: No evidence of phosphine in the atmosphere of Venus from independent analyses. *Nature Astronomy*, *5*, 636-639. doi: 10.1038/s41550-021-01424-x

Greaves, J. S., Richards, A. M. S., Bains, W., Rimmer, P. B., Sagawa, H., Clements, D. L., ... Hoge, J. (2021a, January). Phosphine gas in the cloud decks of Venus. *Nature Astronomy*, *5*, 655-664. doi: 10.1038/s41550-020-1174-4

Greaves, J. S., Rimmer, P. B., Richards, A. M. S., Petkowski, J. J., Bains, W., Ranjan, S., ... Fraser, H. J. (2022, August). Low levels of sulphur dioxide contamination of Venusian phosphine spectra. *MNRAS*, *514*(2), 2994-3001. doi: 10.1093/mnras/stac1438

Klein, B., Hochgürtel, S., Krämer, I., Bell, A., Meyer, K., & Güsten, R. (2012). High-resolution wide-band fast fourier transform spectrometers. *A&A*, *542*, L3. Retrieved from `https://doi.org/10.1051/0004-6361/201218864` doi: 10.1051/0004-6361/201218864

Krasnopolsky, V. A. (1989, July). Vega mission results and chemical composition of Venusian clouds. *Icarus*, *80*(1), 202-210. doi: 10.1016/0019-1035(89)90168-1

Lincowski, A. P., Meadows, V. S., Crisp, D., Akins, A. B., Schwieterman, E. W., Arney, G. N., ... Domagal-Goldman, S. (2021, February). Claimed Detection of PH_3 in the Clouds of Venus Is Consistent with Mesospheric SO_2. *ApJL*, *908*(2), L44. doi: 10.3847/2041-8213/abde47

Mogul, R., Limaye, S. S., Way, M. J., & Cordova, J. A. (2021, April). Venus' Mass Spectra Show Signs of Disequilibria in the Middle Clouds. *GRL*, *48*(7), e91327. doi: 10.1029/2020GL091327

Nixon, C. A., Achterberg, R. K., Teanby, N. A., Irwin, P. G. J., Flaud, J.-M., Kleiner, I., ... Flasar, F. M. (2010, January). Upper limits for undetected trace species in the stratosphere of Titan. *Faraday Discussions*, *147*, 65. doi:

10.1039/c003771k

Pickett, H. M., Poynter, R. L., Cohen, E. A., Delitsky, M. L., Pearson, J. C., & Müller, H. S. P. (1998, November). Submillimeter, millimeter and microwave spectral line catalog. *JQSRT*, *60*(5), 883-890. doi: 10.1016/S0022-4073(98)00091-0

Risacher, C., Güsten, R., Stutzki, J., Hübers, H. W., Aladro, R., Bell, A., ... Wohler, B. (2018, January). The upGREAT Dual Frequency Heterodyne Arrays for SOFIA. *Journal of Astronomical Instrumentation*, *7*(4), 1840014. doi: 10.1142/S2251171718400147

Scargle, J. D. (1982, December). Studies in astronomical time series analysis. II. Statistical aspects of spectral analysis of unevenly spaced data. *ApJ*, *263*, 835-853. doi: 10.1086/160554

Snellen, I. A. G., Guzman-Ramirez, L., Hogerheijde, M. R., Hygate, A. P. S., & van der Tak, F. F. S. (2020, December). Re-analysis of the 267 GHz ALMA observations of Venus. No statistically significant detection of phosphine. *Astron. Astrophys.*, *644*, L2. doi: 10.1051/0004-6361/202039717

Sousa-Silva, C., Seager, S., Ranjan, S., Petkowski, J. J., Zhan, Z., Hu, R., & Bains, W. (2020, February). Phosphine as a Biosignature Gas in Exoplanet Atmospheres. *Astrobiology*, *20*(2), 235-268. doi: 10.1089/ast.2018.1954

Thompson, M. A. (2021, January). The statistical reliability of 267-GHz JCMT observations of Venus: no significant evidence for phosphine absorption. *MNRAS*, *501*(1), L18-L22. doi: 10.1093/mnrasl/slaa187

Trompet, L., Robert, S., Mahieux, A., Schmidt, F., Erwin, J., & Vandaele, A. C. (2021, January). Phosphine in Venus' atmosphere: Detection attempts and upper limits above the cloud top assessed from the SOIR/VEx spectra. *Astron. Astrophys.*, *645*, L4. doi: 10.1051/0004-6361/202039932

Truong, N., & Lunine, J. I. (2021). Volcanically extruded phosphides as an abiotic source of venusian phosphine. *Proceedings of the National Academy of Sciences*, *118*(29), e2021689118. Retrieved from `https://www.pnas.org/doi/abs/10.1073/pnas.2021689118` doi: 10.1073/pnas.2021689118

Villanueva, G. L., Cordiner, M., Irwin, P. G. J., de Pater, I., Butler, B., Gurwell, M., ... Kopparapu, R. (2021, January). No evidence of phosphine in the atmosphere of Venus from independent analyses. *Nature Astronomy*, *5*, 631-635. doi: 10.1038/s41550-021-01422-z

Villanueva, G. L., Smith, M. D., Protopapa, S., Faggi, S., & Mandell, A. M. (2018, September). Planetary Spectrum Generator: An accurate online radiative transfer suite for atmospheres, comets, small bodies and exoplanets. *JQSRT*, *217*, 86-104. doi: 10.1016/j.jqsrt.2018.05.023

Wunderlich, F., Scheucher, M., Grenfell, J. L., Schreier, F., Sousa-Silva, C., Godolt, M., & Rauer, H. (2021, March). Detectability of biosignatures on LHS 1140 b. *Astron. Astrophys.*, *647*, A48. doi: 10.1051/0004-6361/202039663

Zasova, L. V., Moroz, V. I., Linkin, V. M., Khatuntsev, I. V., & Maiorov, B. S. (2006, July). Structure of the Venusian atmosphere from surface up to 100 km. *Cosmic Research*, *44*(4), 364-383. doi: 10.1134/S0010952506040095

Supporting Information for "Phosphine in the Venusian Atmosphere: A Strict Upper Limit from SOFIA GREAT Observations"

M. A. Cordiner[1,2], G. L. Villanueva[1], H. Wiesemeyer[3], S. N. Milam[1], I. de Pater[4], A. Moullet[5], R. Aladro[3], C. A. Nixon[1], A. E. Thelen[1], S. B. Charnley[1], J. Stutzki[3], V. Kofman[1], S. Faggi[1], G. Liuzzi[1,6], R. Cosentino[7], B. A. McGuire[8]

[1]Solar System Exploration Division, NASA Goddard Space Flight Center, 8800 Greenbelt Road, Greenbelt, MD 20771, USA.

[2]Department of Physics, Catholic University of America, Washington, DC 20064, USA.

[3]Max Planck Institute for Radio Astronomy, Auf dem Hügel 69, D-53121 Bonn, Germany.

[4]Department of Astronomy, University of California, 501 Campbell Hall, Berkeley, CA 94720-3411, USA.

[5]NASA Ames Research Center Moffett Field, CA 94035, USA.

[6]School of Engineering, Università degli Studi della Basilicata, 85100, Potenza, Italy

[7]Space Telescope Science Institute, Baltimore, MD 21218, USA.

[8]Department of Chemistry, Massachusetts Institute of Technology, Cambridge, MA 02139, USA.

Contents of this file

1. Table S1.
2. Figures S1 to S3.
3. Supporting Text S1.

Introduction

Table S1 shows the spectral line frequencies, quantum numbers and other spectroscopic parameters for our targeted PH_3 lines.

Figures S1 and S2 illustrate the stepwise (iterative) fringe removal process for the SOFIA 4G1 and 4G2 Venus spectra. Successive steps in the spectral fringe removal process, and the corresponding Lomb-Scargle periodogram at each step, are shown.

Figure S3 shows the final impact of our fringe removal process on the Venus PH_3 spectral models.

Figure S4 shows contribution functions from our radiative transfer model for the PH_3 $J = 1 - 0$ line observed by Greaves et al. (2021a).

Supporting Text S1 describes the origin of the baseline ripples in the calibrated SOFIA 4GREAT spectra.

Table S1. Target PH_3 lines and spectroscopic parameters

Freq. (GHz)	$J''_{K''} - J'_{K'}$	A (s^{-1})	g_u	E_u (K)
533.7946	$2_0 - 1_0$	2.33×10^{-4}	10	38.4
533.8153	$2_1 - 1_1$	1.75×10^{-4}	10	37.7
1066.8359	$4_0 - 3_0$	2.07×10^{-3}	18	128.1
1066.8769	$4_1 - 3_1$	1.94×10^{-3}	18	127.3
1067.0003	$4_2 - 3_2$	1.55×10^{-3}	18	125.0
1067.2063	$4_3 - 3_3$	9.06×10^{-4}	36	121.2

Ref. — JPL Molecular Spectroscopy catalogue (Pickett et al., 1998).

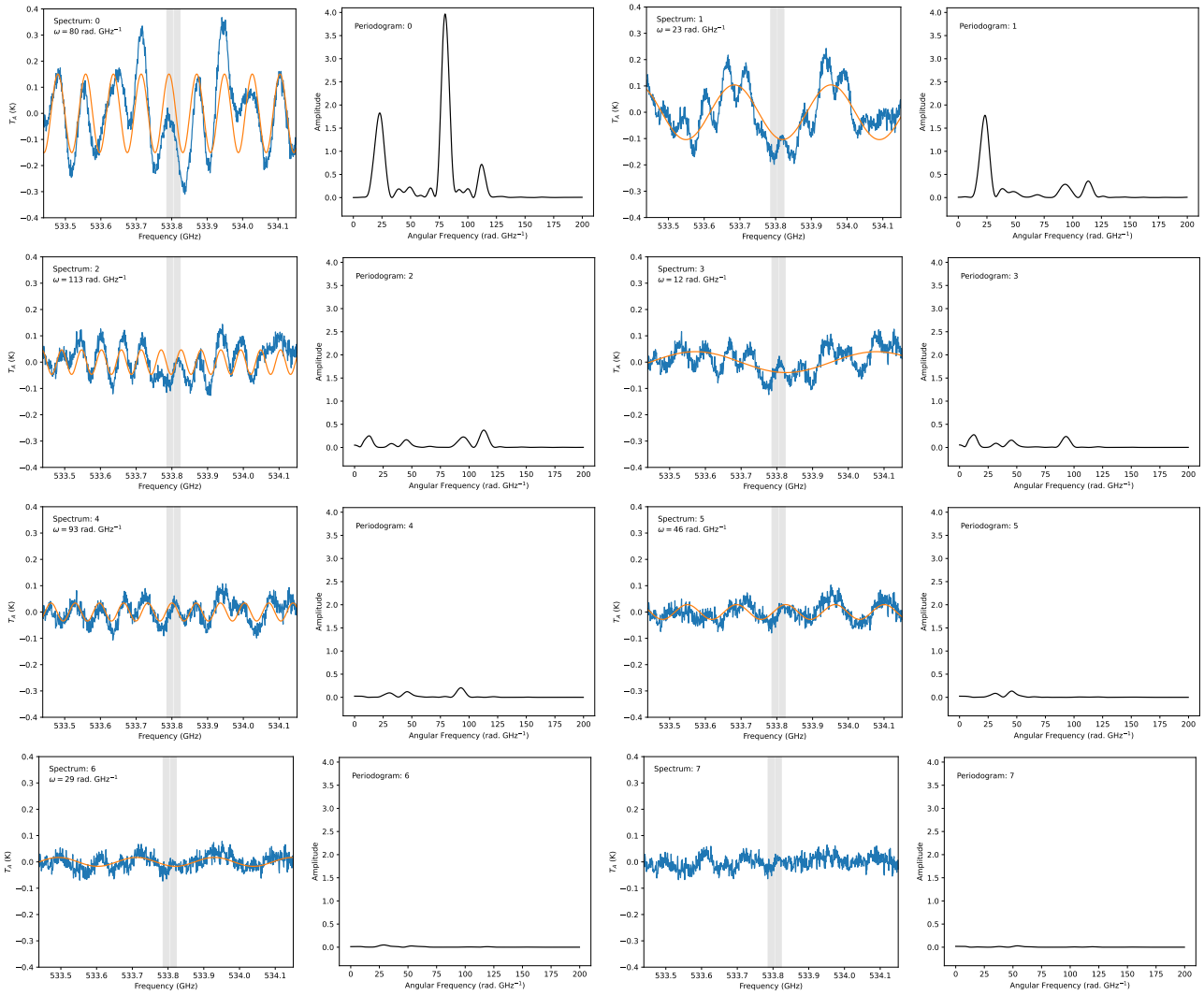

Figure S1. Telluric and continuum-subtracted SOFIA 4G1 Venus spectra (columns 1 and 3), and associated Lomb-Scargle periodograms (columns 2 and 4). Each spectrum represents one iteration of our fringe removal method, up to the final spectrum (lower right), which has 7 periodic fringes removed. Grey bars indicate masked regions around the PH_3 line positions, which were excluded from the periodogram analysis. For each spectral iteration, the observational data are in blue and the fitted sinusoidal fringe is in orange, the angular frequency of which (ω) is given in the upper left.

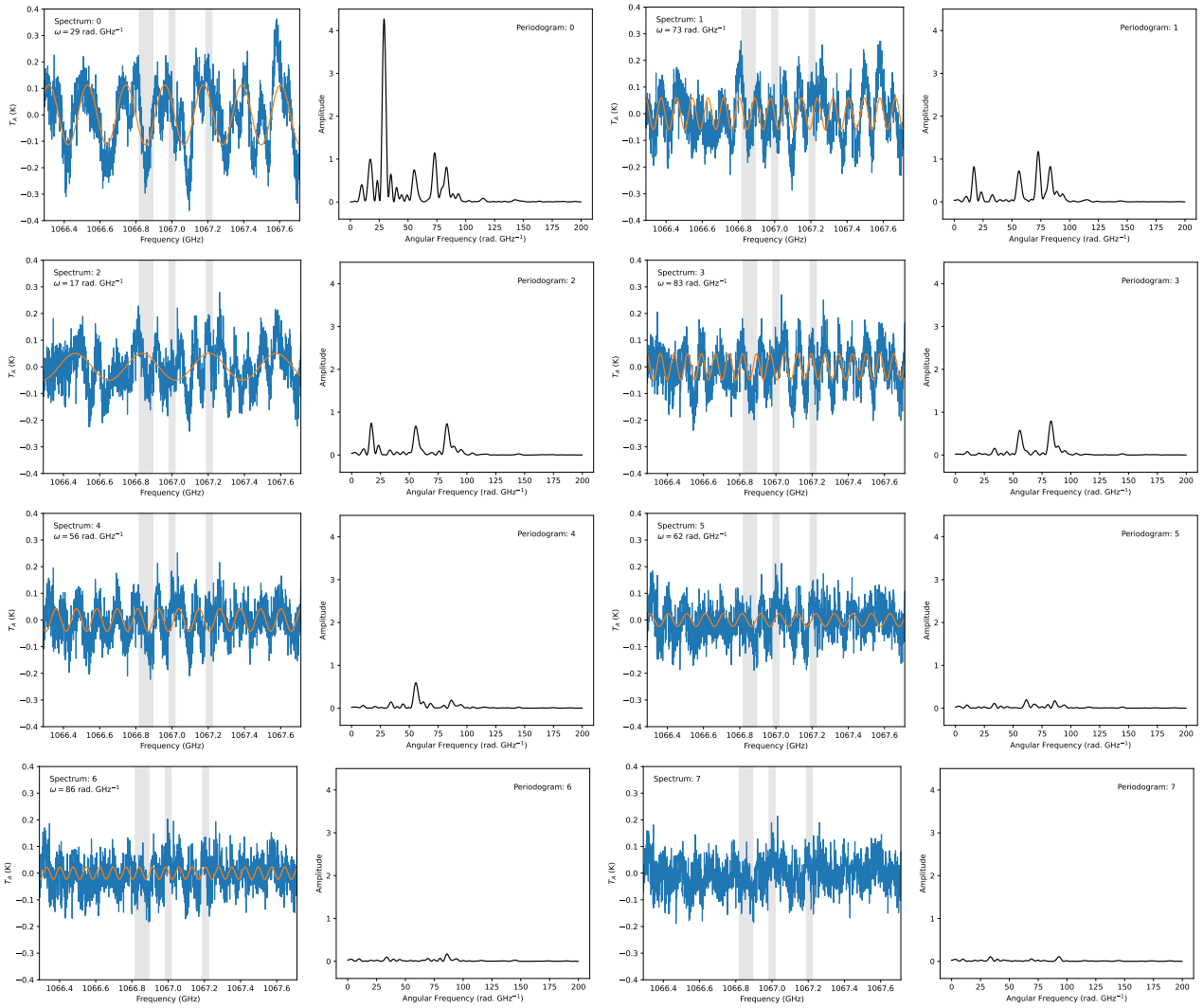

Figure S2. Telluric and continuum-subtracted SOFIA 4G2 Venus spectra (columns 1 and 3), and associated Lomb-Scargle periodograms (columns 2 and 4). Each spectrum represents one iteration of our fringe removal method, up to the final spectrum (lower right), which has 7 periodic fringes removed. Grey bars indicate masked regions around the PH_3 line positions, which were excluded from the periodogram analysis. For each spectral iteration, the observational data are in blue and the fitted sinusoidal fringe is in orange, the angular frequency of which (ω) is given in the upper left.

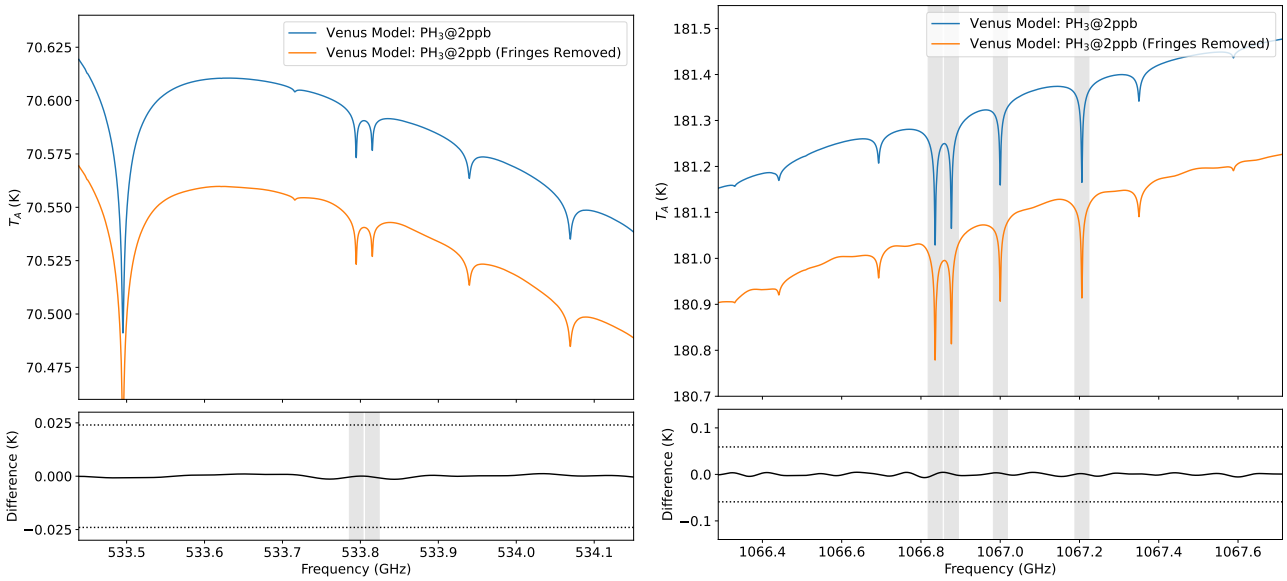

Figure S3. Venus PSG spectral models (blue traces) including PH_3 at a uniform abundance of 2 ppb for 4G1 (left) and 4G2 (right). The orange traces show the spectra after being subjected to the same defringing method as the observed spectra, and have been shifted vertically for display. Lower panels show the difference spectra ('before' minus 'after' defringing), and in both cases, the residual ripples are well below the RMS noise level, which is indicated with dotted lines.

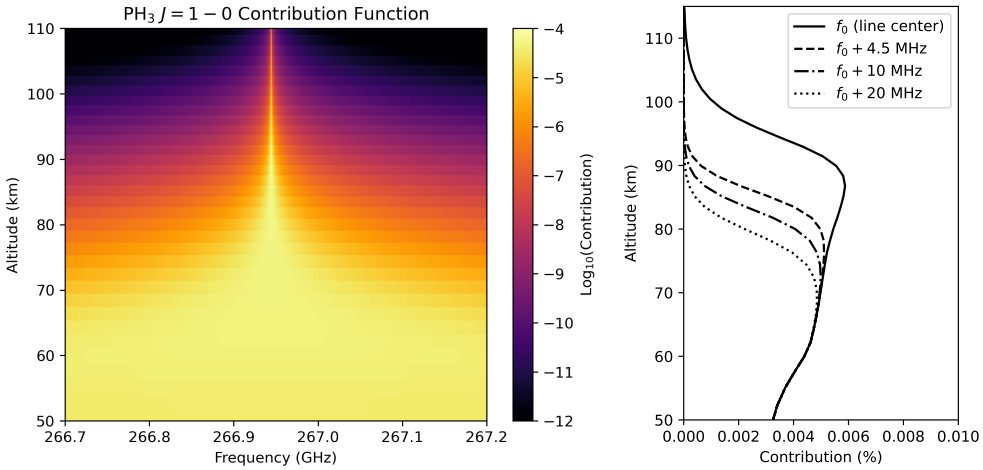

Figure S4. Left panel: contribution function from our Venus radiative transfer model, showing the fraction of the total spectral opacity as a function of frequency and altitude for the PH_3 $J = 1-0$ line observed by Greaves et al. (2021a). Right panel: one-dimensional cuts through the contribution function, at various frequency offsets from the line core frequency (f_0).

S1. Origin of the baseline continuum ripples

Baseline ripples in the 4G1 and 4G2 channels manifest as a quasi-periodic fringe pattern superimposed on the Venus continuum, with an amplitude of about 0.7% of the continuum intensity (see Figure 1 and Figures S1 and S2). These ripples arise from the presence of standing waves between various optical elements of the SOFIA telescope, *e.g.*, the subreflector, and of the 4GREAT instrument with its mixers. The standing waves are additionally modulated by the frequency-dependent (and sideband-dependent) gain profile of the heterodyne instrument, in both the sky frequency and the intermediate frequency domains. As a result of the double-sideband nature of the receiver, and the fact that the power levels in the signal and image sidebands are not exactly matched, the receiver's response to the standing waves is nonlinear, and consequently, they are not fully removed by the spectral calibration procedure, which is expressed by the following equation:

$$\tilde{T}_A = \frac{\tilde{g}_s \circ (\tilde{P}_s^{on} - \tilde{P}_s^{off}) + \tilde{g}_i \circ (\tilde{P}_i^{on} - \tilde{P}_i^{off})}{\tilde{g}_s \circ (\tilde{P}_s^{hot} - \tilde{P}_s^{cold}) + \tilde{g}_i \circ (\tilde{P}_i^{hot} - \tilde{P}_i^{cold})} (T_R^{hot} - T_R^{cold}) \quad (1)$$

In this equation, spectra are denoted as vectors, with $\tilde{P}$ being the total power count rates in the *on* and *off* source positions, or towards the *hot* and *cold* calibration loads, as indexed. Subscripts s and i refer to the signal and image sidebands, respectively, $\circ$ denotes the element-wise (Hadamard) vector product, and $\tilde{T}_A$ is the resulting calibrated spectrum. For simplicity, the above equation assumes that the Rayleigh-Jeans temperatures of the hot and cold loads are equal in both sidebands. Equal count rates (within the noise) in the signal and image bands would result in a flat bandpass, because the gain factors ($\tilde{g}$) cancel. This is indeed the case for the difference between the two off-source beams A and B (located on either side of the optical axis), because in the average total power from A and B (used as the *off* signal for calibrated Venus spectra) it cancels out. Owing to the strong continuum of Venus and its spectral dependence, the gain factors $\tilde{g}_s, i$ no longer cancel, resulting in different total power baseline shapes in the *on* and *off* positions.

Additional harmonics are introduced into the *on* and *off* standing-wave patterns as a result of folding of the waves from the two receiver sideband spectra, which leads to the presence of multiple periodic components, as manifested in the periodograms shown in Figures S1 and S2. Deconvolution of these overlapping (beating) periodic signals is nontrivial, and therefore, a complete physical interpretation/assignment of the periodogram wave frequencies is beyond the scope of the present study.

References

Greaves, J. S., Richards, A. M. S., Bains, W., Rimmer, P. B., Sagawa, H., Clements, D. L., ... Hoge, J. (2021a, January). Phosphine gas in the cloud decks of Venus. *Nature Astronomy*, *5*, 655-664. doi: 10.1038/s41550-020-1174-4

Pickett, H. M., Poynter, R. L., Cohen, E. A., Delitsky, M. L., Pearson, J. C., & Müller, H. S. P. (1998, November). Submillimeter, millimeter and microwave spectral line catalog. *JQSRT*, *60*(5), 883-890. doi: 10.1016/S0022-4073(98)00091-0